Quaternary Science Reviews 80 (2013) 102–111

Contents lists available at ScienceDirect

Quaternary Science Reviews

journal homepage: www.elsevier.com/locate/quascirev

A severe drought during the last millennium in East Java, Indonesia

Jessica R. Rodysill [a, *], James M. Russell [a], Shelley D. Crausbay [b], Satria Bijaksana [c], Mathias Vuille [d], R. Lawrence Edwards [e], Hai Cheng [f, e]

[a] Department of Geological Sciences, Brown University, Providence, RI 02912, USA
[b] Horticulture and Landscape Architecture, Colorado State University, Fort Collins, CO 80523, USA
[c] Faculty of Mining and Petroleum Engineering, Institut Teknologi Bandung, Bandung 40132, Indonesia
[d] Department of Atmospheric and Environmental Sciences, University at Albany, SUNY, 1400 Washington Ave., Albany, NY 12222, USA
[e] Department of Earth Sciences, University of Minnesota, Minneapolis, MN 55455, USA
[f] Institute of Global Environmental Change, Xi'an Jiaotong University, Xi'an 710049, China

ARTICLE INFO

Article history:
Received 1 March 2013
Received in revised form
1 September 2013
Accepted 5 September 2013
Available online

Keywords:
Drought
Indonesia
Indo-Pacific Warm Pool
El Niño-Southern Oscillation
Little Ice Age
Volcanic forcing

ABSTRACT

The Little Ice Age (LIA) is characterized by widespread northern hemisphere cooling during a period of reduced radiative forcing. Sediment records from three crater lakes indicate that the most severe drought of the last 1200 years struck East Java at the end of the LIA. We use ^{14}C and U-series dating applied to carbonate geochemical records from Lakes Lading, Logung, and Lamongan to demonstrate this drought occurred at 1790 Common Era (CE) ± 20 years. Drought occurred during a period of strong El Niño events and Asian monsoon failures in the late 1790s, yet our records indicate that drought conditions persisted well beyond this decade and reached peak intensity in East Java ca 1810 CE ± 30 years. The continuation of severe drought into the 1800s may have resulted from the large volcanic eruptions that occurred in 1809, 1815 and 1835 CE, which likely caused brief, abrupt decreases in Indo-Pacific Warm Pool (IPWP) sea surface temperatures (SSTs), reducing local convection in East Java. Alternatively, broad changes in atmospheric circulation, such as a slowing of the Pacific Walker Circulation in response to decreased solar radiation during the LIA, could have produced several decades of drought in East Java. However, there is a lack of clear supporting evidence for such a change based upon paleohydrological records from the opposite ends of both the Indian and Pacific ocean zonal circulation systems. Based on the available evidence, we suggest severe multidecadal drought in East Java throughout the turn of the 19th century was driven by locally reduced convection resulting from a combination of heightened El Niño activity and volcanic eruptions.

1. Introduction

1.1. Background

Convection over the Indo-Pacific Warm Pool (IPWP) is a major source of atmospheric water vapor and is a vitally important component of the global hydrological cycle (Pierrehumbert, 2000). Emerging records from the IPWP indicate significant hydroclimate changes over the past millennium, which could have important consequences for tropical precipitation and global climate (Crausbay et al., 2006; Griffiths et al., 2009; Oppo et al., 2009; Sachs et al., 2009; Tierney et al., 2010; Rodysill et al., 2012; Konecky et al., 2013). Conflicting trends in reconstructed IPWP hydrology during the Little Ice Age (LIA) call into question how patterns of rainfall and drought respond to extended decadal to millennial-scale periods of warming and cooling. For example, isotopic records from the Makassar Strait and East Java indicate convective activity increased over southern Indonesia through much of the past millennium, yet decadal variations in these records exhibit significant temporal differences in hydrologic extremes (Oppo et al., 2009; Tierney et al., 2010; Rodysill et al., 2012; Konecky et al., 2013).

The Makassar Strait experienced the coldest temperatures of the past millennium circa 1700 CE (Oppo et al., 2009). While cool sea surface temperatures should reduce regional convective activity, lake sediments in East Java record the most severe droughts during the LIA from 1450 to 1650 Common Era (CE) and from 1790 to 1860 CE (Crausbay et al., 2006; Rodysill et al., 2012). These differences could arise from the diverse controls on the intensity of convection in the IPWP, which include changes in the mean position of the Inter-tropical Convergence Zone (ITCZ), changes in IPWP SSTs, and Walker Circulation strength associated with the El Niño-Southern Oscillation (ENSO) or the Indian Ocean Dipole (IOD). Understanding

* Corresponding author. Tel.: +1 401 863 3339.
E-mail address: Jessica_Rodysill@brown.edu (J.R. Rodysill).

0277-3791/$ – see front matter © 2013 Elsevier Ltd. All rights reserved.
http://dx.doi.org/10.1016/j.quascirev.2013.09.005

the regional hydrology in the IPWP during the LIA could illuminate how convective intensity responds to changes in the global climate system, and how IPWP variations in turn affect global-scale climate processes. Here we present a new record of drought from crater lake sediments in East Java and synthesize ages of droughts in nearby crater lakes that provide strong evidence for a major drought in East Java during the LIA.

1.2. Regional setting

Our study site is located between the tropical Indian and Pacific Oceans on the island of Java, Indonesia, just south of the IPWP (Fig. 1A). Seasonal rainfall variations in Java are controlled by the Austral summer monsoon, which brings heavy precipitation from the northwest, and the dry southeasterlies of the Austral winter monsoon (Fig. 1C). Interannual variations in rainfall are influenced by the strength of the monsoons and the phase of ENSO, where anomalous cold SSTs, weaker Walker Circulation, and decreased vertical convection over the IPWP during El Niño events prolong southeasterly flow over Java, lengthening the dry season and causing drought (Hendon, 2003).

Lake Lading (8°0.53′S, 113°18.75′E) is a closed basin lake situated on the southwest side of Gunung Lamongan, a historically active volcano in Eastern Java (Carn and Pyle, 2001; Fig. 1B). This ~200-m-diameter maar crater-lake is 8.6 m deep and sits at an elevation of 324 m in mafic volcanic bedrock (Carn and Pyle, 2001). Observations of water balance and salinity of East Java lakes have shown that lakes in this region are sensitive to seasonal changes in climate (Green et al., 1976), and sediment records from nearby crater lakes have demonstrated that these lakes can preserve a record of climate-driven salinity variations in their lithology and geochemistry covering at least the past 1400 years (Crausbay et al., 2006; Rodysill et al., 2012).

2. Materials and methods

We recovered two cores from the deepest part of Lake Lading using a Bolivia corer in July 2008 in offset, overlapping drives to minimize coring hiatuses. Resistant beds (tephras) below 2.5 m prevented penetration with the Bolivia corer, so a Livingstone coring system was used to recover an additional 3.6 m of sediment. The upper 42 cm of surface sediment was collected with a hand-held Uwitec™ gravity corer and extruded in the field in 1-cm increments with a modified Verschuren (1993) extruder to preserve chemical and physical sediment properties. The cores were split and macroscopically described at Brown University using the methods of Schnurrenberger et al. (2003). These cores were spliced into one composite section by visually correlating distinctive laminae and beds and distinctive geochemical variations.

The core chronology was assembled using ^{210}Pb dating methods to constrain ages in the upper meter of core, and ^{14}C ages on six plant macrofossils and one bulk sediment sample in the lower sections. ^{210}Pb activity was measured using alpha spectroscopy at Flett Research Laboratories, and a constant rate of supply model was used to determine ^{210}Pb ages (Appleby and Oldfield, 1978; Appleby, 1997). Four ^{14}C dates were measured on plant material from cores that were collected from Lading in 1998 (Crausbay, 2000); sample depths corresponding to these dates were correlated to our cores using a combination of visual correlation of distinctive laminae and magnetic susceptibility profiles. An additional three ^{14}C dates were sampled directly from our cores to constrain correlation of the previously measured ^{14}C dates and to fill in gaps in the age model. These samples were analyzed at the Woods Hole Oceanographic Institution's National Ocean Sciences AMS Facility. All of the ^{14}C ages were calibrated to calendar years using the IntCal09 model from Calib 6.0 (Table 1; Stuiver and Reimer, 1993). Two ~20-cm-thick volcanic ash beds were treated as instantaneous events, so we removed them from the composite depth before calculating the age model. The age model and model error approximations were derived using a mixed-effect regression model applied to both ^{210}Pb and calibrated ^{14}C ages (Heegaard et al., 2005).

We developed continuous profiles of the elemental chemistry of our cores using an ITRAX corescanner with a Mo X-ray source at 1-cm resolution with a 120-s dwell time at the University of Minnesota Duluth's Large Lakes Observatory. We also measured the

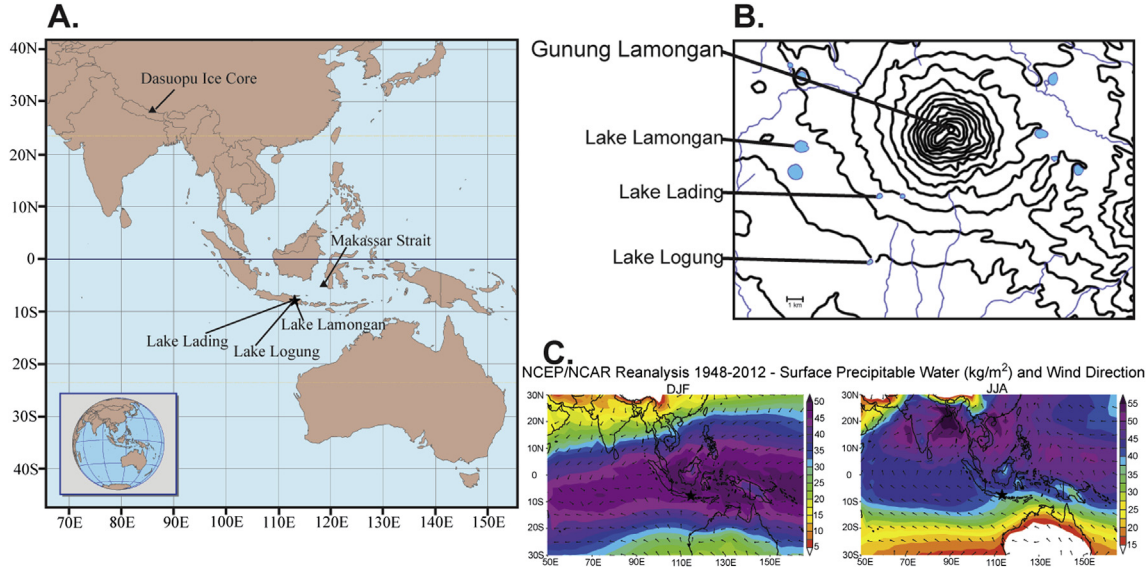

Fig. 1. Location of our study sites and seasonal precipitation maps. **A**: Regional map highlighting the location of our study sites (star) and the Dasuopu ice core and Makassar Strait SST records mentioned in the discussion section (triangles). **B**: Contour map of Gunung Lamongan volcano in East Java with Lakes Lading, Logung, and Lamongan depicted as light blue circles. Black lines are 100 m contours. **C**: Seasonal precipitable water in kg/m^2 and wind direction at 1000 mb in Java during austral summer (left) and austral winter (right). Cooler colors represent a greater amount of precipitable water. (For interpretation of the references to colour in this figure legend, the reader is referred to the web version of this article.)

Table 1
AMS ^{14}C ages on Lake Lading samples are listed in order of increasing cumulative depth with the radiocarbon age and measured age uncertainty (years BP), the calibrated age [year in the Common Era (CE)], and one sigma calibrated age ranges in years CE with their associated probabilities.

Cumulative sediment depth (cm)	Lab sample code	Dated material	^{14}C age (years BP)	Calibrated age (year CE)	1 Sigma age range 1 (years CE) (probability)	1 Sigma age range 2 (years CE) (probability)	1 Sigma age range 3 (years CE) (probability)
178.4	AA37293	Plant/wood	236 ± 30	1790	1644:1668 (0.608821)	1782:1797 (0.364274)	1948:1950 (0.026905)
252.2[a]	OS-79520	Bulk sediment	620 ± 25	1311	1299:1323 (0.40469)	1347:1369 (0.393168)	1380:1392 (0.0.202124)
326.7	AA37294	Plant/wood	412 ± 40	1466	1436:1495 (0.861151)	1602:1615 (0.131489)	1509:1510 (0.007361)
371.1	OS-77312	Plant/wood	690 ± 25	1287	1277:1297 (0.910767)	1373:1377 (0.089233)	
375.6	AA37295	Plant/wood	692 ± 36	1287	1273:1300 (0.741854)	1368:1381 (0.258146)	
433.2	Beta 228346	plant/wood	830 ± 40	1218	1181:1256 (1)		
565.8	OS-77313	Plant/wood	1190 ± 25	845	810:880 (0.898266)	782:790 (0.101734)	

[a] This ^{14}C age was excluded from the age model.

elemental chemistry of the uppermost, extruded sediment using an Innov-X Systems Alpha 4000 XRF. Overlapping measurements of Itrax and Innov-X XRF data have identical trends and were used to scale elemental counts from the Innov-X XRF to those made with the Itrax. Using these data, we estimated calcium carbonate content by normalizing counts of Ca to Ti, assuming that changes in Ti solely reflect terrigenous sources (e.g. Brown et al., 2007; Rodysill et al., 2012). We measured total inorganic carbon (TIC) concentrations on freeze-dried and homogenized subsamples at 10-cm resolution using a UIC CM5014 CO_2 Coulometer with a UIC CM5240 TIC Autoanalyzer to test whether downcore TIC abundance, another measurement that is used to approximate carbonate abundance, shared the same trends as Ca:Ti. Precision on these measurements of 0.237% TIC was verified with pure $CaCO_3$ standards and replication of 10% of the sample measurements. Samples containing greater than 2% TIC were analyzed on a Rigaku MiniFlex X-ray Diffractometer at the University of Minnesota to identify carbonate minerals and estimate percent Mg in calcite using X-ray diffraction (XRD) techniques (Goldsmith and Graf, 1958). We also conducted smear slide analyses across the interval where carbonate is present to characterize the relative abundance and phase of carbonate. Total contents of carbon and nitrogen (TC and TN) were measured, using an NC2100 Elemental Analyzer, on the same set of subsamples on which TIC was measured. Precision of TC and TN analyses is 1.60% and 0.26%, respectively, as determined from standards and replication of 10% of the samples. TIC values were subtracted from TC values to determine the % total organic carbon (TOC), for which the pooled uncertainty is 1.62%. TOC values were then divided by TN values to calculate C:N_{org}. Total organic matter content (% OM) was determined at 1-cm resolution by drying sediment samples in a drying oven overnight at 100 °C, burning the samples for 4 h at 550 °C, and dividing the mass of sample lost by ignition at 550 °C by the dry sediment mass.

We provide additional chronological control on the timing of a drought event documented by carbonate-rich sediment in a core from nearby Lake Lamongan (Crausbay et al., 2006) through absolute dating of lacustrine aragonite with ^{234}U–^{230}Th dating methods (Edwards et al., 1987). Two samples, labeled A and B, from a single bed composed of pure aragonite, as determined by a combination of smear slide analyses and XRD measurements, were analyzed using standard techniques in the Minnesota Isotope Laboratory at the University of Minnesota and are compared to previous ^{14}C-based chronologies from this core.

3. Results

3.1. Core chronology—Lake Lading age model

^{210}Pb and ^{14}C ages indicate that our core from Lake Lading continuously spans the interval from ~800 CE to the present. A ^{14}C date at 371.1 cm from our sediment core is nearly identical to a date from Crausbay's (2000) core taken in 1998, at 375.6 cm in our composite section (Table 1; Fig. 2), demonstrating that the ages obtained in older cores are reproducible and that our correlation of ^{14}C sample depths between cores is accurate. A ^{14}C date at 178.4 cm had multiple possible age ranges with comparable probabilities; we use the age range with the second highest probability, which fit best with sedimentation rates determined from the rest of the ^{14}C ages (Table 1). Using the age range with the highest probability would require a 4-fold increase and decrease in sedimentation rates prior to and during the ^{210}Pb-dated portion of our cores. We do not see evidence in any of our geochemical and lithological data to support such variation in sedimentation, and such changes would be in direct contradiction with the ^{210}Pb age model. The bulk sediment ^{14}C date at 252.2 cm is much older than the rest of the plant macrofossil ^{14}C ages above and below it. Given that there is evidence for reworking of material that resulted in old ^{14}C ages on charcoal and bulk sediment samples from nearby Lake Logung (Rodysill et al., 2012), and the possibility of ^{14}C reservoirs in these systems, we remove this age from the age model. After these adjustments, our mixed-effect regression through six ^{14}C ages between ~800 and 1800 CE indicates roughly linear sedimentation averaging 0.4 cm yr^{-1}, similar to pre-industrial sedimentation rates at nearby Lake Logung (Rodysill et al., 2012). ^{210}Pb data indicate sedimentation rates increase to 1.14 cm yr^{-1} toward the present

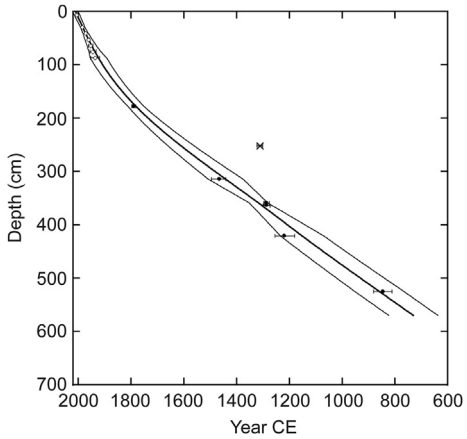

Fig. 2. The Lake Lading age model. ^{14}C ages are shown as dark circles with error bars indicating their associated 1σ errors and ^{210}Pb dates are shown as open diamonds. The ^{14}C age not included in the age model is depicted with an "x." The thick solid line denotes the age model, derived using methods from Heegaard et al. (2005), and the two thin solid lines represent the uncertainty in the age model. The sedimentation rate increases from 0.4 cm/yr below 2 m to 1.14 cm/yr in the ^{210}Pb-dated portion of the core.

(Fig. 2), slightly lower than sedimentation rates during the historical period at Logung (Rodysill et al., 2012).

3.2. Sediment lithology and geochemistry of Lake Lading

Calcium carbonate, estimated from Ca:Ti and % TIC, is nearly absent from Lake Lading sediment except between the late 1700's and early 1800's, when % TIC increases to 6.3% (~ 50% $CaCO_3$) in a set of well-defined lamina (Fig. 3). Our smear slide and XRD-analyses indicate this carbonate is composed of euhedral crystals of calcite, high-Mg calcite (7–8% Mg) and aragonite. Organic matter content ranges between 2 and 25% during the past 1200 years and lacks a clear long-term trend (Fig. 3). $C:N_{org}$ exhibits substantial decadal-scale variability throughout the record, ranging between 10.5 and 19 and gradually decreasing from 1400 CE to the present. There is no clear relationship between either % OM or $C:N_{org}$ and %TIC.

3.3. Lake Lamongan U-series dating

The $^{230}Th/^{238}U$ activity ratio in two aragonite samples from the same depth in Lake Lamongan sediments is very low (0.00256 ± 0.00015 in sample A and 0.00241 ± 0.0005 in sample B), which indicates consistent incorporation of U into the aragonite as it precipitated (Lazar et al., 2004; Table 2). A common problem with using $^{234}U–^{230}Th$ dating methods in sediment samples is the presence of detrital U and Th, which are sources of error in the U–Th date determination (Stein and Goldstein, 2006). Pristine coral aragonite typically has $^{238}U/^{232}Th$ values between 10^4 and 10^5, as compared to aragonite samples from Lake Lisan sediments that contained detrital ^{232}Th and had $^{238}U/^{232}Th$ of $<10^2$ (Stein and Goldstein, 2006). Measured $^{238}U/^{232}Th$ for the two aragonite samples from Lake Lamongan sediments were on the order of 10^3 in sample A and 10^2 in sample B, indicating that sample A had low detrital ^{232}Th relative to sample B. The low $^{238}U/^{232}Th$ likely indicates that the aragonite in that sample contains some detrital ^{232}Th. Maximum ages for samples A and B from the uncorrected ^{230}Th dates are 1732 CE ± 16 years and 1746 CE ± 53 years, respectively (Table 2). Assuming an initial $^{230}Th/^{232}Th$ of $(4.4 \pm 2.2)^{*}10^{-6}$ to correct for the initial ^{230}Th, we calculate an age for sample A of 1774 CE ± 26 years and for sample B of 1791 CE ± 57 years (Table 2). The U-series ages on the aragonite bed from Lake Lamongan give similar ages for the timing of the most severe drought in that reconstruction.

4. Discussion

4.1. Drought in Lake Lading record

Carbonate is present in the sediments of Lake Lading only during a brief, 60-year period within the 1160-year long record, from 1790 to 1850 CE (Fig. 3). The euhedral shape of the calcite and aragonite grains in this bed suggests they are authigenic, indicating that shifts in lake water chemistry and salinity drove carbonate precipitation and preservation. Calcite saturation was most likely achieved by a rise in salinity in response to a decrease in regional precipitation:evaporation (Müller et al., 1972; Kelts and Hsü, 1978). It is unlikely that calcite precipitation was driven by enhanced runoff or groundwater supplying excess Ca^{2+} and HCO_3^-. Carbonate precipitation caused by enhanced runoff and groundwater supply generally occurs as the result of a positive shift in lake water balance in settings where the landscape is a significant source of these ions (Shapley et al., 2005, 2010), but Lake Lading is surrounded by a mafic landscape. Calcite precipitation can also be caused by greater primary productivity that drives CO_2 consumption, which increases the pH and drives the water chemistry to calcite saturation (Kelts and Hsü, 1978). Intensified productivity should increase the delivery of organic matter to the sediments and decrease the $C:N_{org}$, however % OM declines and $C:N_{org}$ is high during the late 1700's-early 1800's when carbonate is present (Meyers and Lallier-Vergès, 1999; Fig. 3). Moreover, XRD and smear slide analyses show that the phase of carbonate throughout this event changes from pure calcite, to a mixture of high Mg-calcite and aragonite, to pure aragonite, then back to a mixture of high Mg-calcite and aragonite, and finally back to pure calcite. The transition from calcite to

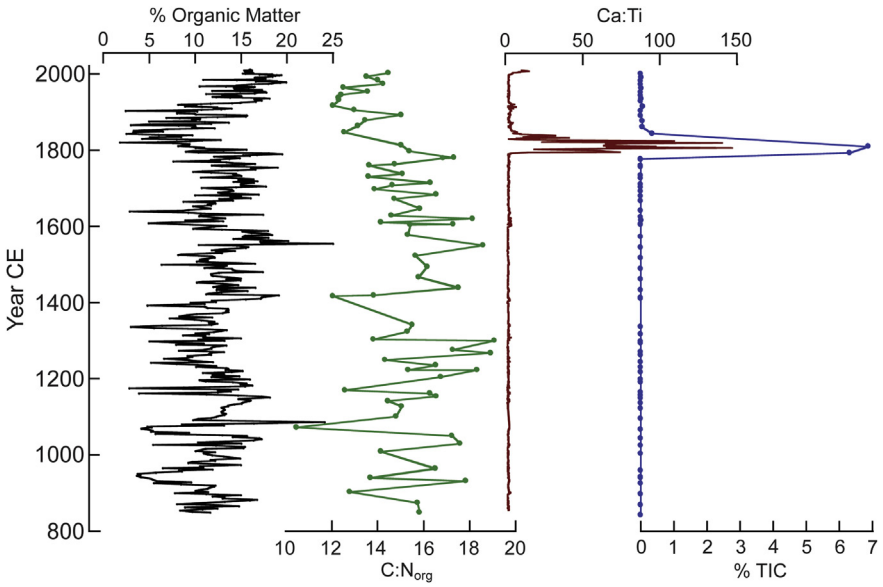

Fig. 3. Lake Lading sediment geochemistry. The left plot is percent organic content determined by loss on ignition (% Organic matter; black), the left middle plot is the ratio of organic carbon to nitrogen ($C:N_{org}$; green), the right middle plot is Ca:Ti calculated from XRF measurements (maroon), and the right plot is percent inorganic carbon (% TIC; blue). Closed circles are individual data points. These data are plotted on a time axis (on the left). (For interpretation of the references to colour in this figure legend, the reader is referred to the web version of this article.)

Table 2
U–Th disequilibrium dating measurements on Lake Lamongan aragonite and associated age corrections.

Sample ID	Sample depth (cm)	^{238}U (ppm) (measured)	^{232}Th (ppb) (measured)	^{230}Th/^{232}Th ($\times 10^{-6}$)	δ^{234}U (measured)	^{230}Th/^{238}U (activity)	^{230}Th date (years CE) (uncorrected)	^{230}Th date (years CE) (corrected)	$\delta^{234}U_{initial}$ (corrected)
A	561.5	6.66 ± 0.03	1.517 ± 0.2	27.9 ± 1.8	49.1 ± 1.9	0.00256 ± 0.00015	1732 ± 16	1774 ± 26	49.1 ± 1.9
B	561.5	8.50 ± 0.20	13.6 ± 1.2	24.3 ± 5.5	46.1 ± 3.2	0.00241 ± 0.0005	1746 ± 53	1791 ± 57	46.1 ± 3.2

aragonite is common in lakes undergoing increasingly evaporative conditions (Müller et al., 1972). Finally, this event is precisely concurrent with the most pronounced enrichment in δD_{wax} data from Lake Lading sediments (Konecky et al., 2013), a completely independent proxy for dry conditions. All of these observations are strong evidence for an evaporatively-driven rise in salinity due to decreased precipitation:evaporation as the primary control on carbonate precipitation in Lake Lading. Our estimate of the age range of this event, 1790–1850 CE, is based upon a mixed-effect regression model (Heegaard et al., 2005) through our ^{14}C and ^{210}Pb ages. Other age modeling techniques provide nearly identical ages; Bacon, for example, gave an age range of 1780–1840 CE (Blaauw and Christen, 2011). Together these data provide robust evidence for drought in East Java between 1790 and 1850 CE.

4.2. Drought in East Java lake records

Lake Lading is one of eleven crater lakes situated near the base of Gunung Lamongan. Among these lakes, Lading, Logung and Lamongan exhibit a clear gradient in calcium carbonate production and preservation. Calcium carbonate is present in the record from Lake Lading between 1790 and 1860 CE and is otherwise absent from the sediments. Four multidecadal periods of carbonate precipitation are present in a sediment core from Lake Logung, and carbonate precipitation was nearly continuous in a core from Lake Lamongan. Despite these geochemical differences, all three records point to the strongest drought conditions of the past millennium during the late 1700s and early 1800s. Drought in Lake Lading lasted from 1790 to 1850, culminating around 1810 CE when calcite was completely replaced by aragonite (Fig. 4A). Our maximum age

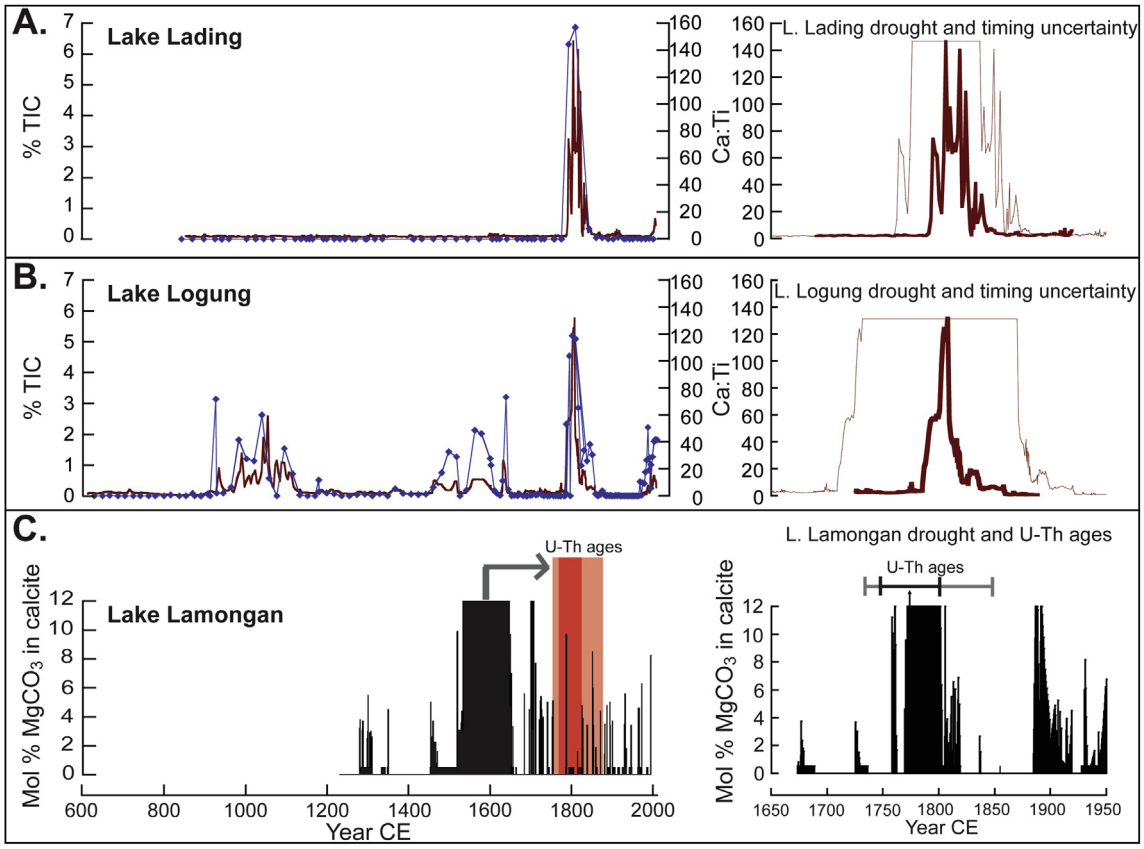

Fig. 4. Drought records from East Java lakes. **A**: On the left, carbonate abundance in Lake Lading is plotted with total inorganic carbon content (% TIC, left axis) displayed in blue circles and Ca:Ti (right axis) displayed in maroon. On the right, Ca:Ti from Lake Lading is plotted in a thick maroon line to show the timing of the late 1700's/early 1800's drought at this site. **B**: On the left, carbonate abundance in Lake Logung (left) is plotted with total inorganic carbon content (% TIC, left axis) displayed in blue circles and Ca:Ti (right axis) displayed in maroon. On the right, Ca:Ti from Lake Logung is plotted in a thick maroon line to show the timing of the late 1700's/early 1800's drought at this site. The earliest onset and latest termination of Ca:Ti in each lake considering maximum age model error is plotted in thin maroon lines to illustrate the maximum age range of the drought. **C**: % $MgCO_3$ in calcite in Lake Lamongan sediments plotted in black on the published age model (left). The arrow points to a dark red rectangle, which represents the U-series age range of Sample A, and a light red rectangle, which represents the U-series age range of Sample B. % $MgCO_3$ in calcite plotted with new ages based upon sedimentation rate between the new U–Th dates (right), shown as black and gray error bars for Sample A and B, respectively, and a core-top age of 1998 CE. The U–Th-dated aragonite lamina is indicated with an arrow. (For interpretation of the references to colour in this figure legend, the reader is referred to the web version of this article.)

error during this event is 30 years, so the drought could have occurred between 1760 and 1880 CE.

The timing of drought in Lake Lading is nearly identical to the timing of a major drought documented in the sediments of Lake Logung, a maar lake 3.5 km south of Lading (Figs. 1B and 4B). Droughts are recorded in Lake Logung by calcium carbonate mineral abundance interpreted from XRF-derived Ca:Ti and % TIC data (Rodysill et al., 2012). The most pronounced rise in calcite abundance in Lake Logung lasts from 1790 to 1860 and reaches maximum abundance between 1800 and 1810 CE (Fig. 4B). The error on this portion of the Lake Logung age model is approximately 70 years, placing the drought between 1720 and 1920 CE. However, the timing of peak carbonate content coincides almost perfectly in the two lakes, suggesting strong drought just after the turn of the 19th century.

Further evidence of drought at this time comes from Lake Lamongan, 5 km northwest of Lake Lading (Fig. 1). Carbonate is more continuously preserved in the sediments of Lake Lamongan, compared with Lakes Lading and Logung, and Crausbay et al. (2006) reconstructed moisture balance in this record from changes in carbonate mineralogy measured by the mol % Mg in calcite from XRD analyses and the phase of carbonate observed in smear slides (Fig. 4C). They estimated that the strongest drought recorded in Lake Lamongan, marked by a prolonged interval of aragonite deposition, occurred at about 1550 CE based upon ^{14}C ages on plant macrofossils. However, lack of ^{210}Pb data, ^{14}C age reversals, plateaus in the ^{14}C age calibration curve during the LIA, and possible stratigraphic discontinuities made the original chronology of the Lamongan record problematic, particularly in the aragonitic section of core indicating drought. Our new U–Th dates obtained near the base of this aragonite bed yielded ages of 1774 CE ± 26 and 1791 CE ± 57 yrs for this interval (Fig. 4C). This implies a much more recent age than was determined through ^{14}C dating at Lamongan, and places the onset of severe drought very close to that observed in nearby Lakes Lading and Logung (~1790 CE ± 30 yrs).

The U–Th ages were sampled from near the base of the aragonite-bearing sediment and therefore mark the beginning of the most severe drought in Lamongan. Interpolating between the U–Th date (1774 CE) and the coretop (1998), an additional 80 cm of aragonite above the U–Th dates represents approximately 40 years of drought after 1774 with a mid-point in the 1790's, roughly in agreement with the length of carbonate-defined droughts in Lakes Lading and Logung. This is a conservative estimate of the duration of the drought in Lamongan; a purely linear sedimentation rate over the last few centuries in this lake is unlikely based on the 3-to-4-fold increases in sedimentation rates in the Lading and Logung basins during the last century (Rodysill et al., 2012; this study). More realistically, aragonite deposition probably persisted well into the 19th century, which would push the middle of the aragonite bed closer to the peak intensity of drought recorded in Lading and Logung ca 1810.

We estimated the timing of peak drought conditions in East Java by calculating a weighted mean age based upon the three records. To do this, we used the U-series age from sample A, which was sampled from the center of the aragonite bed in the Lake Lamongan core, and the ages and associated 95% confidence interval errors at the maximum carbonate concentration in Lakes Lading and Logung predicted from each cores' age model (Fig. 5). The weight assigned to the age from each site is the reciprocal of the variance of each individual age at the 95% confidence level. The weighted mean was calculated by summing the products of the age from each site and their associated weights, then by dividing that value by the sum of the weights. The variance of the weighted mean is the reciprocal of the sum of weights. We determined that the maximum drought intensity in East Java occurred in 1790 CE ± 20 yrs.

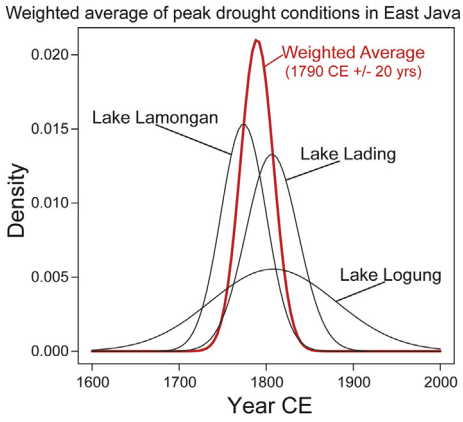

Fig. 5. The probability density functions of the timing of peak drought in each lake and the weighted average age of East Java drought. The black curve from Lake Lamongan is the probability density function of the U-series age on Sample A, the black curve from Lake Lading is the probability density function of the age and 95% confidence interval from the carbonate abundance maximum occurring at 1806.6 CE ± 30 yrs, and the black curve from Lake Logung is the probability density function of the age and 95% confidence interval from the carbonate abundance maximum occurring at 1808 ± 72 yrs. The thick red line is the weighted average age of peak drought conditions in East Java and the variance on the weighted average at the 95% confidence interval. (For interpretation of the references to colour in this figure legend, the reader is referred to the web version of this article.)

In sum, the carbonate content and mineralogy of three crater lakes in eastern Java indicate strong, coherent drought in the late 18th–early 19th century, reaching peak aridity at 1790 CE ± 20 yrs. While Lamongan and Logung show evidence for multiple drought episodes during the past millennium, late 18th–early 19th century is the only event present in the Lake Lading record. The uniqueness of this event in our reconstruction from Lake Lading and its co-occurrence in three separate sites suggests that it was the strongest event to occur in this region during the last millennium.

4.3. Regional climate patterns and mechanisms of late LIA drought in East Java

Drought in East Java can be induced by numerous mechanisms, including a weakening of the Pacific Walker Circulation associated with changes in ENSO and/or the Indian Ocean dipole, a decrease in local convection due to anomalous cooling of IPWP SSTs, and changes in the strength of the Austral-Asian monsoon. Many of these mechanisms operate on seasonal to interannual timescales and their effects are short-lived, such as El Niño and Indian Ocean Dipole (IOD) events. At multidecadal timescales, changes in radiative forcing from volcanism, solar output, and greenhouse gases as well as natural variability in the ocean–atmosphere system might change the nature or frequency of these events and bias their variability toward phases that induce drought in Java. Multidecadal changes in these systems might also arise from changes internal to the Pacific Ocean and/or Indian Ocean circulation and dynamics, of which the long-term patterns and underlying causes are still unclear. Evaluating these forcings and processes and their relationship to late 1700s/early 1800s drought in East Java requires an extremely dense network of high resolution climate proxies. Recent tree ring, lake, and coral records have begun to provide such a framework, and are discussed below.

The East Java Drought peaks in intensity in 1790 CE and lasts approximately six decades. All three of the Indonesian lake records are based upon changes in lake salinity, which exhibits a threshold response to climate changes. Carbonate precipitation does not occur until the lake reaches saturation with respect to calcite, and a

particular phase of carbonate does not stop precipitating until the salinity returns to below that threshold. The prolonged drought in East Java may either represent ~60 years of continually severe drought conditions, or several short-lived extreme droughts occurring in close temporal proximity such that neither the abundance nor phase of carbonate is changed between the termination of one single drought and the start of the next. Arid conditions between short-lived, extreme drought events might have been sustained by soil moisture feedbacks, producing a continuous response to individual stochastic forcing events. While the continuity of drought in East Java during this time is unclear, lake salinity rose to higher levels over the course of the ~60-year arid interval, culminating in peak arid conditions between 1775 and 1810 CE. Whether or not there was a continuous or punctuated decrease in precipitation:evaporation remains unclear. Thus, either a cluster of short-lived droughts during the late 1700s/early 1800s, or a single prolonged drought is capable of producing the signal recorded in the East Java crater lakes.

Tree ring, speleothem, and ice core records from Southeast Asia, India, and Southern Oman have documented numerous droughts in the late 1700s and early 1800s (Thompson et al., 2000; Duan et al., 2004; Fleitmann et al., 2004; Cook et al., 2010). The Strange Parallels Drought lasted from 1756 to 1768 and is associated with a major monsoon failure across India and Southeast Asia (Lieberman, 2003; Cook et al., 2010). The age of the Strange Parallels drought is approximately when prolonged drought began in Lake Lamongan, and is the earliest possible timing of the onset of drought in Lakes Logung and Lading; however, all three lakes indicate that the peak intensity of East Javan drought occurs a few decades after the Strange Parallels drought (Fig. 4). Peak drought conditions in East Java overlap best in timing with the East India Drought, which resulted in widespread aridity in Southeast Asia and India from 1790 to 1796 (Cook et al., 2010). An associated drought in East Java could suggest linkages between Asian Summer Monsoon failure and changes in the Austral-Asian winter monsoon. However, the East India drought was very short-lived relative to the event that we document in East Javan lakes, similar to most droughts documented in Southeast Asian tree-ring archives. Moreover, droughts occurring in Southeast Asia and India were stronger from 1756 to 1768 and 1876 to 1878 (Thompson et al., 2000; Cook et al., 2010) and do not clearly align with peak drought conditions in East Java in the 1790s. Together, these relationships imply that droughts in mainland Asia do not directly correspond to droughts in East Java, so a climatic influence from outside the Asian Monsoon system played a role in creating anomalously dry conditions in East Java from 1790 to 1850 CE (Duan et al., 2004; Cook et al., 2010; Figs. 1 and 5A).

The drought in East Java has perhaps the best temporal association to the "Great El Niño event" between 1789 and 1797, of which the consequences have been documented across much of the tropics (Grove, 2007). This event is thought to include several very strong El Niño years between 1790 and 1796. Historically documented effects include prolonged and severe drought across Australia, the Caribbean islands, Mexico, Egypt, southern Africa, early snowmelt and excessive flooding on the Peruvian coast, and abnormally high temperatures and rainfall in North America (Grove, 1998, 2007; Ortlieb, 2000; Gergis et al., 2010). The earliest of these severe El Niño events coincides with an exceptionally severe drought documented by chloride and dust concentrations and $\delta^{18}O$ in the 560-year-long Himalayan ice core record (Fig. 6A; Thompson et al., 2000). Historical archives of heavy rainfall and fishery failures from Peru document a period of several El Niño events beginning in the late 1700s and persisting into the mid-1800s, making these decades the most active interval of El Niño activity since 1550 in historical records (Garcia-Herrera et al., 2008). It is important to note that there have been individual El Niño events of equal or greater severity between 1525 and 2010 CE documented in historical archives (Ortlieb, 2000) and in the Niño3.4 SST index that do not produce drought in our Lake Lading record. If the Great El Niño caused the drought in East Java, then these data imply that the concentration of several severe El Niño events occurring over a short period of time is capable of producing prolonged East Javan drought, rather than a single, extremely severe El Niño event.

Following the late 1700s Great El Niño Event, a series of several massive volcanic eruptions occurring in 1809, 1815, and 1835 may have acted to prolong the drought in East Java into the early 1800s (Stothers, 1984; D'Arrigo et al., 2006; Cole-Dai et al., 2009). Volcanic eruptions are capable of directly causing drought in the IPWP region by temporarily decreasing IPWP SSTs and locally reducing atmospheric convection. El Niño events also correlate to large volcanic eruptions both in historical and model data (Adams et al., 2003; Mann et al., 2005), and could force drought in East Java through both local and remote ocean–atmosphere interactions. Large eruptions have been previously invoked to explain extreme declines in western Pacific warm pool SSTs between 1808 and 1818 CE and between 1836 and 1838 CE (D'Arrigo et al., 2006; Fig. 6B). Peak carbonate abundance in the Lake Lading and Logung records occurs from 1800 to 1820 CE, slightly later than peak aridity in the Lake Lamongan record. Differences in the timing of peak aridity between the three crater lakes may result from age model uncertainties or differing sensitivities of the geochemistry at each site to changes in local aridity, as discussed in Section 4.2. The latter could imply aridity in East Java continued into the early 1800s, overlapping with the two large volcanic eruptions and the coldest IPWP SSTs in the early 1800s. Another volcanic eruption in 1835 CE occurred at the same time as another sharp drop in reconstructed IPWP SSTs, and may have contributed to drought after 1815 CE (Fig. 6B; D'Arrigo et al., 2006).

Interannual drought in East Java is influenced not only by ENSO and volcanic activity but also zonal circulation changes in the Indian Ocean associated with the Indian Ocean Dipole mode. Positive IOD events are associated with reduced convection and drought in the IPWP region and enhanced convection and precipitation over the western Indian Ocean and East Africa (Ashok et al., 2004). A recent modeling study demonstrated that, on multi-decadal timescales, Indian Ocean SSTs alter the Indian Ocean Walker Circulation and drive multi-decadal precipitation anomalies in East Africa in the absence of a Pacific Ocean influence (Tierney et al., 2013; Fig. 6C). If either IOD activity or multidecadal "IOD-like" SST anomalies in the Indian Ocean caused East Javan drought, we would expect drought in East Java to correlate to positive rainfall anomalies along the east coast of tropical Africa. Based on our reconstruction, however, drought in East Java coincides with declining precipitation in East Africa (Tierney et al., 2013; Fig. 6C). Similar evidence for drought in East Africa during this time period comes from Lake Naivasha (Verschuren et al., 2000) and Challa (Wolff et al., 2011). These records strongly suggest that East Africa was dry during drought in East Java, suggesting these events do not arise from IOD-like mechanisms. Our study sites in East Java are influenced by both Indian and Pacific ocean-atmosphere systems, and it is possible that changes in convection over the Indian Ocean may not have a significant impact on east Javan precipitation if the Pacific ocean-atmosphere system is unchanged. Whatever the case may be, this evidence suggests that neither prolonged positive IOD-like conditions persisting for several decades nor an increase in the frequency or intensity of interannual IOD events throughout the late 1700s/early 1800s were responsible for drought in East Java.

The association between drought in East Java, the Great El Niño Event, and volcanic eruption-induced cooling of warm pool SSTs

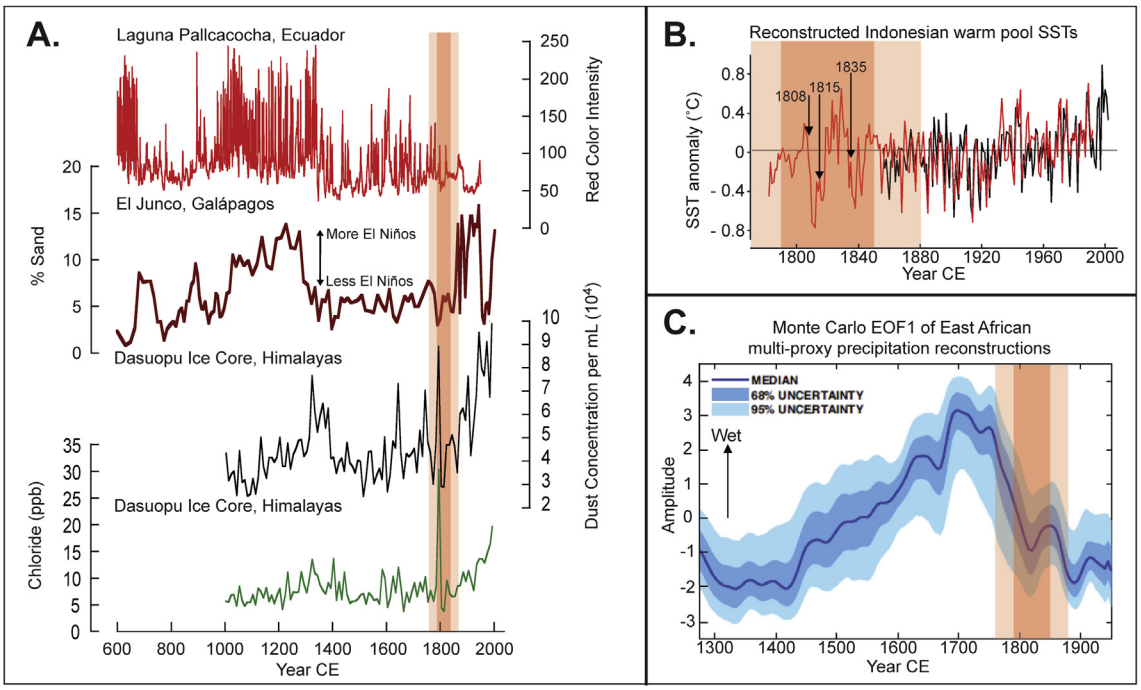

Fig. 6. Comparison of Lake Lading drought and relevant paleoclimate records. **Panel A**: From top to bottom the records shown are Laguna Pallcacocha, Ecuador red color intensity (red, Moy et al., 2002), El Junco Lake, Galápagos % sand (maroon, Conroy et al., 2008), and the Dasuopu ice core dust (black) and chloride (green) concentrations (Thompson et al., 2000). Drought in Lake Lading sediments does not occur during any substantial El Niño activity inferred from EEP records, but does begin at the same time as drought inferred from the Himalayan ice core data. The timing of the drought in Lake Lading (1790–1850 CE) is indicated by a dark red rectangle, with the age uncertainty (1760–1790 and 1850–1880 CE) indicated by a light red rectangle. Note that these age ranges are for the Lake Lading drought only, and Lake Lamongan U–Th ages suggest the onset of drought in that basin may have occurred earlier than 1790 (~1775) CE. **Panel B**: Instrumental Indonesian warm pool SSTs are shown in black and reconstructed SSTs, based on tree ring and coral data, are shown in red; modified after D'Arrigo et al. (2006). The volcanic eruptions occurring in 1809, 1815, and 1835 are highlighted with arrows. The timing of the drought in Lake Lading (1790–1850 CE) is indicated by a dark red rectangle, with the age uncertainty (1760–1790 and 1850–1880 CE) indicated by a light red rectangle. Anomalously cold SSTs span the decade during which the volcanic eruptions occurred and are concurrent with drought in Lake Lading sediments. **Panel C**: The dark blue thin line is the Monte Carlo EOF1 produced in the study by Tierney et al. (2013) which indicates a prolonged pluvial during the 17th–19th centuries. 68% and 95% age uncertainty in the EOF output are shown as medium and light blue shading. Drought in Lake Lading, illustrated by the darker red rectangle, begins at the tail end of this pluvial, and persists beyond it into the mid-1800's. The lighter red rectangle illustrates the uncertainty in the timing of the drought in Lake Lading. (For interpretation of the references to colour in this figure legend, the reader is referred to the web version of this article.)

strongly implicates changes in the tropical Pacific Walker Circulation as the forcing behind East Javan drought. If so, we would expect to find evidence for enhanced runoff in climate reconstructions on the eastern limb of the Pacific Walker Circulation. However, lake sediment runoff records from the Galápagos and Ecuador, a record of $\delta^{18}O$ from Galápagos corals, and South American ice core records in the Eastern Equatorial Pacific (EEP) region, which is climatically sensitive to historical ENSO activity, do not provide evidence for heightened El Niño activity or wet conditions at multi-decadal timescales during the late 1700s/early 1800s (Fig. 6A; Dunbar et al., 1994; Moy et al., 2002; Thompson et al., 2003; Conroy et al., 2008). In fact, lake sediment records from the Galápagos exhibit the lowest frequency of runoff events in the last four centuries in the early 1800s, and Ecuadorian lake sediment records indicate very few runoff events throughout the drought in East Java. Given the extensive historical documentation of multiple intense El Niño events during the 1790s, it is possible that the spatial distribution of El Niño-driven precipitation anomalies may have been different during the 1790s relative to the present, such that the decade of severe El Niño events was not documented in these paleoreconstructions.

Drought in East Java was not driven by the multi-century decrease in western Pacific SST that occurred in the context of the LIA because the coldest SSTs occurred in the early 1700s, nearly a century before drought in our record (Oppo et al., 2009). It is possible that the East Java drought is a manifestation of random local variability, perhaps associated with cool SSTs and generally weakened atmospheric convection over the IPWP during the LIA. We find this explanation unlikely given that an internal random variable would need to coincide, by chance, with a series of extraordinarily strong volcanic eruptions and high frequency of El Niño events. This drought may then more likely be the result of several short-lived events (e.g. El Niño events, volcanic eruptions) that, while common throughout the last millennium, happened to occur in close timing during the late 1700's and early 1800's to produce a uniquely long and severe drought in an ENSO, IOD, and monsoon sensitive region such as East Java.

5. Conclusions

The strongest drought in East Java of the past millennium occurred at ~1790 CE ± 20 yrs, during a prolonged period of cool IPWP SSTs during the late Little Ice Age. New U–Th dates pin the peak intensity of the drought to the late 1700s, and evidence for dry conditions from three crater-lake records suggests the drought was regionally coherent and severe, persisting well into the mid-1800s. It is clear from the synchronous onset of the drought in lakes Lading, Lamongan and Logung, within age model uncertainties, that dry conditions began in East Java in the late 1700s and peaked in intensity at 1790 CE ± 20 years, coinciding with a series of globally-documented severe El Niño events between 1789 and 1797 termed the "Great El Niño event." The persistence of the East Java drought until 1850 CE ± 30 years, and peak drought intensity lasting through 1810 CE, may have been driven by three large

volcanic eruptions at 1809, 1815, and 1835 CE, which set up conditions for drought through short-lived cooling of IPWP SSTs. While each of these climate drivers tends to produce drought on seasonal to interannual timescales, we suggest a combination of many short-lived drought-inducing events occurring in close temporal proximity to one another produced many decades of severe drought in East Java.

Acknowledgments

We thank the Government of Indonesia and Indonesian Ministry of Research and Technology (RISTEK) for permission and assistance in conducting field research. We thank Ed Cushing for providing ^{14}C ages from Lake Lading. We also thank Dave Murray, Joe Orchardo, and Candice Bousquet for laboratory assistance, Jessica Tierney, Kevin Anchukaitis, and Bronwen Konecky for improving the quality of this project, and the Limnological Research Center. This research was supported by a NOAA-CCDD grant to J. Russell and M. Vuille.

References

Adams, J.B., Mann, M.E., Ammann, C.M., 2003. Proxy evidence for an El Niño-like response to volcanic forcing. Nature 426, 274–278.
Appleby, P.G., 1997. Sediment records of fallout radionuclides and their application to studies of sediment–water interactions. Water Air Soil Pollut. 99, 573–586.
Appleby, P.G., Oldfield, F., 1978. The calculation of ^{210}Pb dates assuming a constant rate of supply of unsupported ^{210}Pb to the sediment. Catena 5, 1–8.
Ashok, K., Guan, Z., Saji, N.H., Yamagata, T., 2004. Individual and combined influences of ENSO and the Indian Ocean Dipole on the Indian Summer Monsoon. J. Clim. 17, 3141–3155.
Blaauw, M., Christen, J.A., 2011. Flexible paleoclimate age–depth models using an autoregressive gamma process. Bayesian Anal. 6, 457–474.
Brown, E.T., Johnson, T.C., Scholz, C.A., Cohen, A.S., King, J.W., 2007. Abrupt change in tropical African climate linked to the bipolar seesaw over the past 55,000 years. Geophys. Res. Lett. 34, L20702. http://dx.doi.org/10.1029/2007GL031240.
Carn, S.A., Pyle, D.M., 2001. Petrology and geochemistry of the Lamongan volcanic field, east Java, Indonesia: primitive Sunda Arc magmas in an extensional tectonic setting? J. Petrol. 42, 1643–1683.
Cole-Dai, J., Ferris, D., Lanciki, A., Savarino, J., Baroni, M., Thiemens, M.H., 2009. Cold decade (AD 1810–1819) caused by Tambora (1815) and another (1809) stratospheric volcanic eruption. Geophys. Res. Lett. 36, L22703. http://dx.doi.org/10.1029/2009GL040882.
Conroy, J.L., Overpeck, J.T., Cole, J.E., Shanahan, T.M., Steinitz-Kannan, M., 2008. Holocene changes in eastern tropical Pacific climate inferred from a Galápagos lake sediment record. Quat. Sci. Rev. 27, 1166–1180.
Cook, E.R., Anchukaitis, K.J., Buckley, B.M., D'Arrigo, R.D., Jacoby, G.C., Wright, W.E., 2010. Asian monsoon failure and megadrought during the last millennium. Science 328, 486–489.
Crausbay, S.D., 2000. A High-resolution Record of Climate and Lowland Vegetation over the Past Millennium in East Java (MS. thesis). Dept. of Ecology, University of Minnesota, Minneapolis, MN, p. 123.
Crausbay, S.D., Russell, J.M., Schnurrenberger, D.W., 2006. A ca. 800-year lithological record of drought from sub-annually laminated lake sediment, East Java. J. Paleolimnol. 35, 641–659.
Duan, K., Yao, T., Thompson, L.G., 2004. Low-frequency of southern Asian monsoon variability using a 295-year record from the Dasuopu ice core in the central Himalayas. Geophys. Res. Lett. 31, L16209. http://dx.doi.org/10.1029/2004GL020015.
Dunbar, R.B., Wellington, G.M., Colgan, M.W., Glynn, P.W., 1994. Eastern Pacific sea surface temperature since 1600 A.D.: the $\delta^{18}O$ record of climate variability in Galápagos corals. Paleoceanography 9, 291–315.
D'Arrigo, R., Wilson, R., Palmer, J., Krusic, P., Curtis, A., Sakulich, J., Bijaksana, S., Zulaikah, S., Ngkoimani, L.O., Tudhope, A., 2006. The reconstructed Indonesian warm pool sea surface temperatures from tree rings and corals: linkages to Asian monsoon drought and El Niño-Southern Oscillation. Paleoceanography 21, PA3005. http://dx.doi.org/10.1029/2005PA001256.
Edwards, R.L., Chen, J.H., Wasserburg, G.J., 1987. ^{238}U-^{234}U-^{230}Th-^{232}Th systematics and the precise measurement of time over the past 500,000 years. Earth Planet. Sci. Lett. 81, 175–192.
Fleitmann, D., Burns, S.J., Neff, U., Mudelsee, M., Mangini, A., Matter, A., 2004. Palaeoclimatic interpretation of high-resolution oxygen isotope profiles derived from annually laminated speleothems from Southern Oman. Quat. Sci. Rev. 23, 935–945.
Garcia-Herrera, R., Diaz, H.F., Garcia, R.R., Prieto, M.R., Barriopedro, D., Moyano, R., Hernández, E., 2008. A chronology of El Niño events from primary documentary sources in northern Peru. J. Clim. 21, 1948–1962.
Gergis, J., Garden, D., Fenby, C., 2010. The influence of climate on the first European settlement of Australia: a comparison of weather journals, documentary data and palaeoclimate records, 1788–1793. Env. Hist. 15, 485–507.
Goldsmith, J.R., Graf, D.L., 1958. Relation between lattice constants and composition of the Ca–Mg carbonates. Am. Miner. 43, 84–101.
Green, J., Corbet, S.A., Watts, E., Lan, O.B., 1976. Ecological studies on Indonesian lakes. Overturn and restratification of Lake Lamongan. J. Zool. 180, 315–354.
Griffiths, M.L., Drysdale, R.N., Gagan, M.K., Zhao, J.-X., Ayliffe, L.K., Hellstrom, J.C., Hantoro, W.S., Frisia, S., Feng, Y.-X., Cartwright, I., St. Pierre, E., Fischer, M.J., Suwargadi, B.W., 2009. Increasing Australian–Indonesian monsoon rainfall linked to early Holocene sea-level rise. Nat. Geosci. 2, 636–639.
Grove, R.H., 1998. Global impact of the 1789–93 El Niño. Nature 393, 318–319.
Grove, R.H., 2007. The Great El Niño of 1789–1793 and its global consequences: reconstructing an extreme climate event in world environmental history. Mediev. Hist. J. 10. http://dx.doi.org/10.1177/097194580701000203.
Heegaard, E., Birks, H.J.B., Telford, R.J., 2005. Relationships between calibrated ages and depth in stratigraphical sequences: an estimation procedure by mixed-effect regression. Holocene 15, 612–618.
Hendon, H.H., 2003. Indonesian rainfall variability: impacts of ENSO and local air-sea interaction. J. Clim. 16, 1775–1790.
Kelts, K., Hsü, K.J., 1978. Freshwater carbonate sedimentation. In: Lerman, A. (Ed.), Lakes: Chemistry, Physics, Geology. Springer-Verlag, New York, pp. 295–323.
Konecky, B.L., Russell, J.M., Rodysill, J.R., Vuille, M., Bijaksana, S., Huang, Y., 2013. Intensification of southwestern Indonesian rainfall over the past millennium. Geophys. Res. Lett. 40. http://dx.doi.org/10.1029/2012GL054331.
Lazar, B., Enmar, R., Schossberger, M., Bar-Matthews, M., Halicz, L., Stein, M., 2004. Diagenetic effects on the distribution of uranium in live and Holocene corals: examples from the Gulf of Aqaba. Geochim. Cosmochim. Acta 68, 4583–4593. http://dx.doi.org/10.1016/j.gca.2004.03.029.
Lieberman, V., 2003. Strange Parallels: Southeast Asia in Global Context, C. 800–1830. In: Integration on the Mainland. Cambridge University Press, Cambridge.
Mann, M.E., Cane, M.A., Zebiak, S.E., Clement, A., 2005. Volcanic and solar forcing of the tropical Pacific over the past 1000 years. J. Clim. 18, 447–456.
Meyers, P.A., Lallier-Vergès, E., 1999. Lacustrine sedimentary organic matter records of Late Quaternary paleoclimates. J. Paleolimnol. 21, 345–372.
Moy, C.M., Seltzer, G.O., Rodbell, D.T., Anderson, D.M., 2002. Variability of El Niño/Southern Oscillation activity at millennial timescales during the Holocene epoch. Nature 420, 162–165.
Müller, G., Irion, G., Förstner, U., 1972. Formation and diagenesis of inorganic Ca–Mg carbonates in the lacustrine environment. Naturwissenschaften 59, 158–164.
Oppo, D.W., Rosenthal, Y., Linsley, B.K., 2009. 2,000-year-long temperature and hydrology reconstructions from the Indo-Pacific Warm Pool. Nature 460, 1113–1116.
Ortlieb, L., 2000. The documented historical record of El Niño events in Peru: An update of the Quinn record sixteenth through nineteenth centuries. In: Diaz, Henry F., Markgraf, Vera (Eds.), El Niño and the Southern Oscillation: Multiscale Variability and Global and Regional Impacts. Cambridge University Press, Cambridge, pp. 207–295.
Pierrehumbert, R.T., 2000. Climate change and the tropical Pacific: the sleeping dragon wakes. Proc. Natl. Acad. Sci. 97, 1355–1358.
Rodysill, J.R., Russell, J.M., Bijaksana, S., Brown, E.T., Safiuddin, L.O., Eggermont, H., 2012. A paleolimnological record of rainfall and drought from East Java, Indonesia during the last 1,400 years. J. Paleolimnol. 47, 125–139.
Sachs, J.P., Sachse, D., Smittenberg, R.H., Zhang, Z., Battisti, D., Golubic, S., 2009. Southward movement of the Pacific intertropical convergence zone AD 1400–1850. Nat. Geosci. 2, 519–525.
Schnurrenberger, D., Russell, J.M., Kelts, K., 2003. Classification of lacustrine sediments based on sedimentary components. J. Paleolimnol. 29, 141–154.
Shapley, M.D., Ito, E., Donovan, J.J., 2005. Authigenic calcium carbonate flux in groundwater-controlled lakes: implications for lacustrine paleoclimate records. Geochim. Cosmochim. Acta 69, 2517–2533.
Shapley, M.D., Ito, E., Forester, R.M., 2010. Negative correlations between Mg:Ca and total dissolved solids in lakes: false aridity signals and decoupling mechanisms for paleohydrologic proxies. Geology 38, 427–430.
Stein, M., Goldstein, S.L., 2006. U–Th and radiocarbon chronologies of late Quaternary lacustrine records of the Dead Sea basin: methods and applications. Geo. Soc. Am. Spec. Pap. 401, 141–154.
Stothers, R.B., 1984. The Great Tambora eruption in 1815 and its aftermath. Science 224, 1191–1198.
Stuiver, M., Reimer, P.J., 1993. Extended ^{14}C data base and revised Calib 3.0 ^{14}C age calibration program. Radiocarbon 35, 215–230.
Thompson, L.G., Yao, T., Mosley-Thompson, E., Davis, M.E., Henderson, K.A., Lin, P.-N., 2000. A high-resolution millennial record of the south Asian monsoon from Himalaya Ice Cores. Science 289, 1916–1919.
Thompson, L.G., Mosley-Thompson, E., Davis, M.E., Lin, P.N., Henderson, K., Mashiotta, T.A., 2003. Tropical glacier and ice core evidence of climate change on annual to millennial timescales. Clim. Chang. 59, 137–155.
Tierney, J.E., Oppo, D.W., Rosenthal, Y., Russell, J.M., Linsley, B.K., 2010. Coordinated hydrological regimes in the Indo-Pacific region during the past two millennia. Paleoceanography 25, PA1102. http://dx.doi.org/10.1029/2009PA001871.
Tierney, J.E., Smerdon, J.E., Anchukaitis, K.J., Seager, R., 2013. Multidecadal variability in East African hydroclimate controlled by the Indian Ocean. Nature 493, 389–392.

Verschuren, D., 1993. A lightweight extruder for accurate sectioning of soft-bottom lake sediment cores in the field. Limnol. Oceanogr. 38, 1796–1802.
Verschuren, D., Laird, K.R., Cumming, B.F., 2000. Rainfall and drought in equatorial East Africa during the past 1,100 years. Nature 403, 410–414.
Wolff, C., Haug, G.H., Timmermann, A., Sinninghe Damsté, J.S., Brauer, A., Sigman, D.M., Cane, M.A., Verschuren, D., 2011. Reduced interannual rainfall variability in East Africa during the Last Ice Age. Science 333, 743–747.